



Published in final edited form as:

Life Sci Space Res (Amst). 2015 July ; 6: 21–28. doi:10.1016/j.lssr.2015.06.003.

Dermatopathology effects of simulated solar particle event radiation exposure in the porcine model

Jenine K. Sanzari¹, Eric S. Diffenderfer¹, Sarah Hagan¹, Paul C. Billings¹, Daila S. Gridley², John T. Seykora³, Ann R. Kennedy¹, and Keith A. Cengel¹

¹Department of Radiation Oncology, Perelman School of Medicine, University of Pennsylvania, Philadelphia, PA 19104

²Department of Radiation Medicine, Radiation Research Laboratories, Loma Linda University and Medical Center, Loma Linda, CA 92354

³Department of Dermatology, Perelman School of Medicine, University of Pennsylvania, Philadelphia, PA 19104

Abstract

The space environment exposes astronauts to risks of acute and chronic exposure to ionizing radiation. Of particular concern is possible exposure to ionizing radiation from a solar particle event (SPE). During an SPE, magnetic disturbances in specific regions of the Sun result in the release of intense bursts of ionizing radiation, primarily consisting of protons that have a highly variable energy spectrum. Thus, SPE events can lead to significant total body radiation exposures to astronauts in space vehicles and especially while performing extravehicular activities. Simulated energy profiles suggest that SPE radiation exposures are likely to be highest in the skin. In the current report, we have used our established miniature pig model system to evaluate the skin toxicity of simulated SPE radiation exposures that closely resemble the energy and fluence profile of the September, 1989 SPE using either conventional radiation (electrons) or proton simulated SPE radiation. Exposure of animals to electron or proton radiation led to dose-dependent increases in epidermal pigmentation, the presence of necrotic keratinocytes at the dermal-epidermal boundary and pigment incontinence, manifested by the presence of melanophages in the dermis upon histological examination. We also observed epidermal hyperplasia and a reduction in vascular density at 30 days following exposure to electron or proton simulated SPE radiation. These results suggest that the doses of electron or proton simulated SPE radiation results in significant skin toxicity that is quantitatively and qualitatively similar. Radiation-induced skin damage is often one of the first clinical signs of both acute and non-acute radiation injury where infection may occur, if not treated. In this report, histopathology analyses of acute radiation-induced skin injury are discussed.

Corresponding author: Jenine K. Sanzari, Department of Radiation Oncology, University of Pennsylvania School of Medicine, 183 John Morgan Building, Philadelphia PA 19104-6072, w: 215.898.5088, f: 215.898.1411, Sanzari@mail.med.upenn.edu.

Publisher's Disclaimer: This is a PDF file of an unedited manuscript that has been accepted for publication. As a service to our customers we are providing this early version of the manuscript. The manuscript will undergo copyediting, typesetting, and review of the resulting proof before it is published in its final citable form. Please note that during the production process errors may be discovered which could affect the content, and all legal disclaimers that apply to the journal pertain.

Introduction

NASA is planning exploration class missions that are expected to involve space travel over periods of months to years. The space radiation environment exposes astronauts to risks of acute and chronic exposure to ionizing radiation. Of particular concern is exposure to ionizing radiation in a solar particle event (SPE). In an SPE, magnetic disturbances in specific regions of the Sun result in the release of intense bursts of ionizing radiation, primarily consisting of protons that have a highly variable energy spectrum [1-5]. Especially during space travel missions outside of the protection afforded by the Earth's magnetosphere, the risks of radiation dose absorbed from SPE exposure are a serious concern for astronauts spending extended time in the space environment. It is estimated that during an SPE event, astronauts conducting extravehicular activities (EVAs) could receive radiation doses to the skin which are 10fold higher than doses to internal organs [6]. Based on SPE events taking place in 1972 and 1989, skin doses to astronauts conducting EVAs were predicted to range from 7-32 Gy [2]. Additionally, SPEs are difficult to forecast in advance. This makes the goal of accurately predicting the biological effects for SPE exposed astronauts even more critical so that potential adverse events can be anticipated and strategies for their mitigation can be developed.

Ionizing radiation has well documented effects on skin. Much of our current understanding of radiation-induced skin damage has been gleaned from animal experiments using beta radiation and x-rays and in humans, from patients receiving radiation therapy and fluoroscopically guided interventional procedures [7, 8]. In addition, a body of literature is limited, but available on normal tissue responses, specifically, radiation-induced skin injury after accidental radiation exposure. Adverse skin reactions can manifest a range of toxicities from inflammatory damage, as evidenced by erythema, hyperpigmentation, edema/hyperproliferation, moist desquamation (skin thins and begins to weep), epilation (hair loss), dermal atrophy, and necrosis that may require surgical intervention. The time course and recovery from radiation damage to skin depends on the total dose and dose rate or fractionation schedule. Areas of skin that have apparently healed following acute damage can subsequently develop severe late effects including necrosis, dermal atrophy and other problems that largely relate to deterioration or collapse of the skin vasculature. In addition, sufficiently severe acute effects may never completely heal, with the potential consequence of leading to sub-acute damage and consequential late effects, including morbidity [9, 10].

Structurally, pig skin is very similar to human skin [8]. The skin is organized into 3 primary layers: epidermis, dermis and hypodermis [11, 12]. The epidermal layer is further subdivided into five layers or stratum: basale (basal, lowest), spinosum (spinous or prickle cell), granulosum (granular), lucidum (clear) and outermost corneum (horny). The relative thickness of the stratum corneum varies depending upon the anatomical location from which the skin was derived. The dermis, which sits below the epidermis, is comprised of two layers: a superficial papillary dermis and a thicker, reticular dermis. Directly below the dermis resides the hypodermis, which is primarily composed of subcutaneous fat. Pigs are frequently used as a model system in dermatological research as their skin responds to radiation exposure in a similar manner to that observed in humans. The pig model has been used previously to determine the response of skin to beta particles, neutrons, x-rays and

heavy ions [13-17]. However, there is very limited information available regarding the acute effects resulting from total body exposure to simulated SPE radiation. Previously it has been demonstrated that electron simulated SPEs can be used as a form of standard reference radiation for these studies [18] and evaluated the toxicity of a relatively superficial electron simulated SPE in a porcine model [15]. In the current report, an extension of the previous studies was conducted by evaluating the acute skin response of Yucatan miniature (mini-) pigs following total body exposure to either electron or proton radiation that specifically mimics the September 1989 SPE. Proton or electron radiation was utilized matching the fluence/energy profiles expected during historically recorded SPEs. Because the macroscopic depth dose distributions for eSPE and pSPE are matched closely, the acute effects from exposure to these two different types of radiation could be directly compared in these studies. Skin samples taken from animals before and after radiation exposure were analyzed over a 30 day time frame, as this is the approximate turnover time for skin [19, 20].

One aim of this study was to determine the relative biological effectiveness (RBE) values for acute effects produced by proton simulated SPE radiation exposure compared to those effects produced by electron simulated SPE radiation (used as the standard, reference radiation). Here we describe histological findings in mini-pigs exposed to electron or proton simulated SPE total body irradiation, referred to as eSPE or pSPE, respectively, from this point forward.

Materials and Methods

Animals

Yucatan mini-pigs were obtained from Sinclair BioResources (Columbia, MO). The pigs ranged from 8-14 weeks old. Pigs were fed standard mini-pig chow two times daily and water *ad libitum*, and maintained on a standard 12 hr light/dark cycle. Animals were given daily enrichment activities and randomly placed in treatment groups of 3 animals per group (8 groups total). All animals and procedures carried out in this study were conducted under protocols approved by the University of Pennsylvania and Loma Linda University Medical Center (LLUMC) Institutional Animal Care and Use Committees.

Irradiation

All radiation exposures were given as total body irradiation (TBI). The types and doses of radiation used were designed to mimic SPE conditions and to represent the radiation environment which astronauts would realistically be exposed to in space [2, 6, 18].

For the eSPE radiation exposures procedures, non-anesthetized animals (8-14 weeks of age) were placed in rectangular plexiglass cages [75 cm (L) × 32.5 cm (H) × 30 cm (D); 0.5 cm thick wall]. The animals were irradiated with a mixture of energies (6 + 12 MeV) consisting of 80% 6 MeV electrons, relative to $d_{\max} = 11$ mm and 20% 12 MeV electrons, relative to $d_{\max} = 26$ mm, at total body doses of 5 Gy (1.7 Gy/hr), 7.5 Gy (2.5 Gy/hr), and 10 Gy (3.3 Gy/hr) [18]. The dose rate was not constant amongst the different dose exposures. ESPE irradiation was produced by a Clinac iX linear accelerator (LINAC; Varian Medical Systems) located in the Perelman Center for Advanced Medicine, University of

Pennsylvania, at a source-to-skin distance of 5 m (see Table 1). The cages were rotated 180° every 25% dose and surface patient dosimetry verification devices (OneDose, Sixel Technologies, Morrisville, NC) were used to confirm the skin doses received. Animals were irradiated or sham-irradiated over a 3 hour exposure period.

A separate cohort of animals was exposed to pSPE radiation. For these experiments, a custom designed double scattering system was developed to allow delivery of a 50 cm diameter radiation field with a radiation flatness (dose uniformity) 3.5% or better. This system was installed on the research beamline at LLUMC and was tuned to deliver a dose of approximately 5 Gy/hr. A clinical modulator wheel was used to create a fully modulated 155 MeV/n proton beam, while radiation dose was prescribed at a depth of 1.1 cm in water along the central beam axis. A 2 stage bolus at the level of the animal chamber and beam weighting allowed for generation of a custom depth dose profile to match the combined 6 + 12 MeV electron beam, which itself was developed to mimic the dose profile of SPE protons (Fig. 1). This setup delivered a maximum proton range of 5.0 cm (approximately 80 MeV) at the entrance of the animal cage and a distribution of proton energies below 80 MeV (due to beam modulation), which is reflective of the space environment where the maximum proton energy is accompanied by a significant number of lower energy protons. The dose at the prescription point was calibrated using an Exradin T1 ionization chamber. Animals received total doses to the skin of 5.0, 7.7 or 10.0 Gy at a constant dose rate with the animal cage rotated at 50% dose delivery per side and dose delivery was verified with thermoluminescent dosimeters that were attached to the animals. A complete description of the proton radiation and dosimetry procedures are described previously [21]. The dose profiles for 6 + 12 MeV electrons and SPE-like protons were modeled using a Monte Carlo simulation (Fig. 1).

Coronal slices from computed tomography (CT) images of mini-pigs were overlaid with a dose heat map generated by Monte Carlo simulation software [22]. The dose deposition profile is consistent between the eSPE and pSPE dosimetry profiles with ~100% of the dose deposited within 10mm from the surface of the skin.

Skin Analyses

All animals were observed daily following the radiation (or sham-irradiation) exposures. Irradiated animals consistently experienced increased skin pigmentation, analogous to a tanning response. To quantify this response, skin pigmentation in animals was scored daily for 30 days using color-coded cards, and the pigs were given a pigmentation score from lightest (1, white) to darkest (8, black) as previously described [15]. Three consistent (amongst each animal) sections were scored against the color-coded cards and the scores were averaged. Next, average scores from each animal were combined to calculate the average score from the 3 animals per radiation dose group at each time point.

Two skin punch biopsy (3-4 mm) samples were obtained from anesthetized animals prior to irradiation (Pre) and 7, 14, and 30 days post-irradiation (7d, 14d, 30d, respectively) and immediately placed in buffered formalin for fixation. The time frame chosen was based on the fact that skin turnover is approximately 30 days in humans and 14 days in rodents [19]. One fixed biopsy sample obtained from the equivalent areas amongst all animals was

embedded in paraffin for histological analysis. Tissue embedding, sectioning and staining was performed by the Histology Core A in the Department of Dermatology, Perelman School of Medicine. Paraffin sections were stained with Hematoxylin/Eosin (HE) or Fontana-Masson, for visualization of melanin.

Stained sections from all animals were evaluated by a board certified dermatopathologist (Dr. John Seykora), for assessment of pathological changes over the designated time course. The criteria used for assessing radiation-induced skin changes included the degree of epidermal pigmentation and pigment incontinence (as indicated by the presence of melanophages in the dermis), the presence of necrotic keratinocytes, the degree of epidermal cell proliferation and changes in the stratum corneum (parakeratosis). Melanophages were manually counted and presented as the number of melanophages/100 μm^2 .

The melanin content in histological sections was quantified using optical imaging software, similar to previously described [23]. Briefly, photomicrographs of Fontana Masson stained sections (at 40 \times) were imported into GIMP- GNU Image Manipulation Program (Link: www.gimp.org). Using GIMP, positively stained melanin granules were demarcated and the resulting image was subsequently imported into ImageJ software (rsbweb.nih.gov/ij). The number of pixels in the demarcated melanin-containing areas was summed and corrected for the width of each section to provide an estimate of the amount of melanin. This technique is described in detail by Billings et al. [24].

Immunohistochemistry (KI67 and Histone H2AX staining)

Tissue sections were heated at 68°C for 45 min, deparaffinized in xylene and rehydrated. For staining with the KI67 (antigen strictly associated with proliferation) antibody (Abcam, Cambridge, MA), antigen retrieval was performed by placing slides in 0.01M sodium citrate buffer (pH 6.0) and gently heating the slides in buffer for 10 minutes. Slides were developed with DAB following the vendor's protocol (3,3'-Diaminobenzidine, EXPOSE mouse and rabbit specific HRP/DAB detection IHC immunohistochemistry kit; Abcam). The sections were blocked with Abcam Protein Block for 30minutes and rinsed twice in TBS, then stained with Ki67 antibody (Abcam ab16667) diluted 1:250 in TBS+BSA (TBS, 0.1% Tween 20, 1% BSA) and incubated overnight at 4° in a humidified chamber to prevent drying. Sections were washed, exposed to a secondary antibody (anti-rabbit-HRP) for 1 hour at room temperature, washed, incubated with DAB solution for 10 minutes at room temperature, counterstained with Ehrlich's Hematoxylin, dehydrated in successive increasing concentrations of ethanol, starting with two water rinses and ending in two xylene rinses, and mounted with Vectamount and allowed to dry.

Staining for phosphorylated Histone H2AX (γ -H2AX) followed a similar procedure as above, except sections were blocked in PBTG (1M glycine, 1% BSA, and 0.1% Triton \times in PBS) for 45 minutes at room temperature and then rinsed briefly in PBS. The sections were incubated with anti-phospho-Histone H2AX (Millipore 05-636) diluted 1:500 in PBTG for 1 hour at 37°C. After several washes, sections were incubated with Alexa Fluor 488 goat anti-Mouse secondary antibody (Life Technologies A11029) diluted 1:600 in PBTG for 35minutes at 37°, washed, and mounted with VectaShield mounting media with DAPI.

Image Analysis (KI67 and γ -H2AX staining)

γ -H2AX stained slides were captured on a Nikon Eclipse TE2000-U fluorescence microscope (Nikon, Tokyo, Japan) using a 15 \times objective lens. Image Pro Plus 7.0 software (Media Cybernetics, Rockville, MD, USA) was used to analyze multiple digital images. that were manually analyzed for the presence of γ -H2AX foci/nucleus. The results are shown as the percent of γ -H2AX positively-stained nuclei.

KI67 stained slides were digitally scanned using the 20 \times objective using a Scanscope OS slide scanner (Leica Biosystems Imaging, Inc. Vista, CA). The total number of cells and the number of Ki67 positively stained cells were recorded using Aperio ImageScope software (Leica Biosystems, Wetzlar, Germany). Results are shown as the percent of positively stained cells per frame.

Results

The baseline skin color of normal Yucatan mini-pigs used in these studies was whitish-grey. We previously established a skin scoring system for grading radiation-induced hyperpigmentation in mini-pigs using a graded scale from 1 (lightest) to 8 (darkest) [15] and applied this system for the present analysis. Skin hyperpigmentation or the “tanning response” was evident as early as 7 days post-irradiation (either eSPE or pSPE exposure) and persisted throughout the 30 day experimental time period. Animals exposed to eSPE radiation exhibited a radiation dose-dependent pigmentation response (Fig. 2). The pSPE radiation resulted in similar skin color changes when comparing the animals exposed to the 5 Gy and 7.7 Gy doses, with the largest increase in pigmentation after the 10 Gy dose exposure.

Changes in skin biopsy samples were evaluated on days 7, 14 and 30 following exposure to eSPE or pSPE radiation. HE stained skin biopsy sections from animals exposed to either 10 Gy eSPE or pSPE radiation at 14 and 30 days post-irradiation (as well as the corresponding pre-irradiation baseline section) are shown in Figure 3. By 14 days post-radiation exposure, increased pigmentation in the basal layer was observed with increased melanin deposition extended into the stratum granulosum, evidenced by the brown pigment in the HE stained sections (Fig. 3B, 3E), supporting the gross observation of skin hyperpigmentation. The presence of necrotic keratinocytes were observed at the dermal-epidermal junction in biopsy samples taken at the 7d and 14d time points (black arrows, Fig. 3B & 3E, 7d images not shown), compared to the pre-irradiation samples in both the eSPE and pSPE treated animals. Random parakeratin was present in the stratum corneum (outermost layer) in most animals exposed to the eSPE radiation. Also evident were random shrunken (pyknotic) residual nuclei (rectangular box, Fig. 3C) in the keratin layer of some of the eSPE samples. The presence of the parakeratin was not consistently present in the pSPE-exposed animals.

Skin hyperpigmentation was supported by the increased melanin deposition, confirmed in Fontana Masson stained sections (Fig. 4), compared to the sections collected at the pre-irradiation time point (Pre, Fig. 4A, 4D). Fontana Masson stained slides were used to quantify the levels of increased pigmentation in the 5 Gy and 10 Gy dose groups, resulting in statistically significant increases in melanin staining at the 14 day time point (Fig. 5).

Scattered melanophages, indicative of pigment incontinence (abnormal transfer of melanin from epidermal cells to the dermis), were present and remained localized around superficial dermal vessels (representative images after the 10 Gy dose exposures to eSPE or pSPE radiation shown in Figures 6B, 6C) at 30 days following eSPE or pSPE radiation exposure. ESPE and pSPE radiation induced a significant increase in the number of melanophages present, compared to pre-irradiated sections (Fig. 6D).

The radiation-induced increase in dermal melanophages to calculate the relative biological effectiveness (RBE) values for pSPE radiation. The number of dermal melanophages increased exponentially with increasing radiation dose in animals irradiated with eSPE or pSPE. RBE values for eSPE or pSPE inducing increased melanophage numbers were determined and exhibited a downward trend with increasing proton dose (Fig. 6). The lower limit of the 95% confidence interval of the RBE at a proton dose of 5 Gy was above 1.0, indicating the pSPE was significantly more effective in increasing the melanophage number, compared with the eSPE radiation. The 95% confidence intervals for RBE determinations include 1.0 at 7.7 and 10 Gy (Table 2), indicating that pSPE radiation exposure was not significantly different from eSPE radiation exposure (i.e., the RBE was not significantly different than 1.0) at increasing melanophage numbers in this dose range.

It is widely accepted that ultraviolet rays induce DNA damage in the skin. Ionizing radiation effects on skin injury are limited to *in vitro* and small animal model systems. Recently, Ahmed et al. reported DNA damage in mini-pigs exposed to localized gamma radiation, using large doses of 50 Gy [17]. DNA damage/repair was detected in the skin of irradiated pigs on day 7 post-irradiation by phosphorylated γ -H2AX staining. A statistically significant increase in the percentage of nuclei positively stained for γ -H2AX was observed in both the eSPE and pSPE irradiated animals, compared to the pre-irradiation control values (Fig. 8).

Increased expression of the proliferation marker, KI67 was observed by day 14 post-radiation. Staining was performed in the pSPE-exposed animals at either the 5 Gy or 10 Gy dose. KI67 expression was increased in a statistically significant manner (Fig. 9), compared to the KI67 staining in the pre-irradiated skin biopsies.

Discussion

In this report, the acute dermatopathology effects (up to 30 days post-irradiation) of pSPE and eSPE radiation on pig skin were investigated. Histopathological analyses of skin biopsies reveal increased melanin deposition, increased proliferation of the epidermis (increased expression of the proliferation marker KI67), parakeratosis, and an increased presence of melanophages within 30 days of ionizing radiation exposure. The present findings suggest that ionizing radiation induces an inflammatory response in the skin after total body irradiation. Further, DNA damage/repair is observed as late as 7 days post-irradiation in both the proton and electron-exposed animals, which may be a useful biomarker in the skin of exposed individuals.

At the gross level, animals exposed to eSPE or pSPE radiation experienced a hyperpigmentation response, which was clearly observed by day 7 following radiation

exposure. Results from histopathologic analysis confirmed increased pigmentation in the stratum basal level of the epidermis by day 7 post-radiation, which extended into the stratum spinosum by day 14 post-radiation, when the level of hyperpigmentation was most intense. By day 30, pigmentation extended throughout the epidermis (not just the basal layer) and into the stratum corneum. Melanin staining was highest at day 14 post-irradiation, with weak staining by day 30 post-irradiation. Additionally, by day 30, the melanin is also ingested by melanophages, as the number of melanophages present increased with dose (of either pSPE or eSPE radiation). The increase in melanophage number is consistent with pigment incontinence and often noted in inflammatory diseases, including melasma and post-inflammatory hyperpigmentation, suggesting that the induction of melanophage recruitment observed here is associated with radiation-induced responses of the cutaneous immune system. The calculated RBE values for melanophage number was > 1.0 at a proton dose of 5 Gy, but approached 1.0 at the higher doses. In summary, electron and proton radiation exposure both increase epidermal pigmentation and pigment incontinence in an acute manner as evidenced by changes in radiation-induced melanin trafficking. The important question of whether melanin production protects against radiation-induced DNA damage is debateable [25, 26].

Skin pigmentation is a complex process involving over 150 genes [11, 12, 27] and much of our current understanding of pigmentation has been gleaned from studies examining the effects of ultraviolet (UV) radiation on skin [27-30]. At this time, it is not known whether similar mechanisms are involved with ionizing radiation-induced pigmentation. DNA damage in skin cells is believed to play an important role in the pigmentation response [11, 12]. DNA damage is observed in the skin of both the eSPE and pSPE irradiated animals as late as 7 days post-radiation, in response to moderate doses of radiation, indicated by H2AX phosphorylation. Our histopathologic findings are compatible with post-inflammatory hyperpigmentation, which is characterized by increased melanin production observed in response to a variety of skin damaging agents [29, 30], followed by a hyperproliferative response. In addition, the results reported here are also consistent with the delayed tanning response induced specifically by UV-B radiation exposure, as opposed to the UV-A induced immediate tanning response described by Costin and Hearing [11], which resolves approximately 3 to 24 hours after UV-A exposure. If indeed the hyperpigmentation response of electron or proton ionizing radiation exposure is similar to that of UV-B radiation exposure, it is possible that the molecular mechanism(s) of UV-B induced DNA damage in the skin is also consistent, potentially resulting in various skin cancers.

Parakeratin (in the stratum corneum) was consistently observed in eSPE-exposed animals, but it was only present in some of the pSPE-exposed animals. Parakeratosis, or the presence of flattened keratinocyte nuclei within the stratum corneum, is often observed in inflammatory skin diseases such as eczema or psoriasis or in tumorous diseases. Mild epidermal hyperplasia/thickening was also observed as increased KI67 staining was present following radiation exposure, confirming that eSPE and pSPE exposure induces a hyperproliferative response in skin. Abnormal epidermal thickening is common in a variety of inflammatory conditions [31]. The histopathology described here is indicative of an inflammatory state consistent with a recent report on SPE-like radiation-induced inflammation and subsequent altered skin immune function in mini-pigs and mice [32].

Earlier studies by Hopewell [8], Lippincott et. al. [13], van den Aardweg et. al. [14], Zacharias et. al. [16] and more recently Ahmed et al. [17] exposed localized areas of skin to high doses of radiation. The current study used whole body radiation exposure which involved skin doses considerably lower than those utilized in the earlier work cited above. If the high doses utilized in the previous skin studies were given as whole body doses, the radiation doses would have been lethal to the animals. The skin doses used in these studies were designed to be considerably larger than the internal organ doses resulting from whole body irradiations, as expected for SPE radiation exposure [18].

The skin doses evaluated in this study are lower than some of those estimated for astronauts, who could have been exposed to SPE radiation during major SPEs in the past. The total skin doses estimated for astronauts during EVAs, as predicted from modeling two different historical SPEs, are 32.15 Gy (for the August 1972 SPE) and 25.99 Gy (for the October 1989 SPE [2]). Astronauts will receive SPE radiation as a whole body dose (as opposed to the relatively small areas of the body exposed to radiation during interventional radiology procedures). Further, astronauts will be exposed daily to higher doses of other types of space radiations (e.g. galactic cosmic rays) which are not encountered on Earth. Additionally, astronauts may be exposed to multiple SPE doses of radiation, which is anticipated to incur a higher degree of skin injury than what is reported here.

This is the first study examining the response of pig skin following acute total body exposure to simulated proton SPE radiation. The changes associated with radiation-induced hyperpigmentation and skin thickening, in response to SPE radiation, are similar to those described for UV-B radiation exposure that ultimately can lead to skin cancer, but further molecular characterization is warranted. Taken together, the acute effects of ionizing radiation to the skin described here may trigger events of a larger inflammatory response, which may be of particular concern after multiple exposures during fractionated radiotherapy schedules or during deep space missions.

Acknowledgments

This work was funded by the National Space Biomedical Research Institute (NSBRI) through NASA NCC 9-58, the Skin Diseases Research Core Center (SDRC) 5-P30-AR-057217, NIAMS, and the National Institutes of Health Radiation Biology Training Grant T32CA009677.

The authors would like to thank Dr. Gabriel Krigsfeld, Ms. Molly Peterlin, Ms. Alexandria Savage, Dr. Salman Punekar, Dr. Casey Maks and Dr. Shalini Mehrotra for helpful technical assistance with the animal procedures, Mr. Leroy Ash and Dr. Stephen M. Prouty for assistance with the tissue processing and staining, and lastly Dr. Andrew Wroe, Mr. Steven Rightmar, Mr. Pete Koss, Mr. Celso Perez and the rest of the Loma Linda University Medical Center Accelerator Team for their expert assistance with the proton irradiation procedures.

References

1. Hellweg CE, Baumstark-Khan C. Getting ready for the manned mission to Mars: the astronauts' risk from space radiation. *Naturwissenschaften*. 2007; 94:517–26. [PubMed: 17235598]
2. Hu S, Kim MH, McClellan GE, Cucinotta FA. Modeling the acute health effects of astronauts from exposure to large solar particle events. *Health Phys*. 2009; 96:465–76. [PubMed: 19276707]
3. Smart DF, Shea MA. Comment on estimating the solar proton environment that may affect Mars missions. *Adv Space Res*. 2003; 31:45–50. [PubMed: 12577924]

4. Townsend LW. Implications of the space radiation environment for human exploration in deep space. *Radiat Prot Dosimetry*. 2005; 115:44–50. [PubMed: 16381680]
5. Wilson JW, Cucinotta FA, Shinn JL, Simonsen LC, et al. Shielding from solar particle event exposures in deep space. *Radiat Res*. 1999; 30:361–82.
6. Wu H, H J, Casey R, Kim MH, Cucinotta FA. Risk of acute radiation syndromes due to solar particle events. Human Research Program Requirements Document, HRP-47052, Rev C. 2009:171–190.
7. Balter S, Hopewell JW, Miller DL, Wagner LK, et al. Fluoroscopically guided interventional procedures: a review of radiation effects on patients' skin and hair. *Radiology*. 2010; 254:326–41. [PubMed: 20093507]
8. Hopewell JW. The skin: its structure and response to ionizing radiation. *Int J Radiat Biol*. 1990; 57:751–73. [PubMed: 1969905]
9. RicKS, R.; Fry, SA. The medical basis for radiation accident preparedness II. New York, Amsterdam, London: Elsevier Science Ltd; 1991.
10. I.A.E. Agency. , editor. Radiological accident in Goiania. Austria: 1988.
11. Costin GE, Hearing VJ. Human skin pigmentation: melanocytes modulate skin color in response to stress. *Faseb Journal*. 2007; 21:976–94. [PubMed: 17242160]
12. Yamaguchi Y, Brenner M, Hearing VJ. The regulation of skin pigmentation. *J Biol Chem*. 2007; 282:27557–61. [PubMed: 17635904]
13. Lippincott SW, Wilson JD, Montour JL. Radiation effects on pig skin. Exposure to different densities of ionization. *Arch Pathol*. 1975; 99:105–10. [PubMed: 1115680]
14. van den Aardweg GJ, Hopewell JW, Simmonds RH. Repair and recovery in the epithelial and vascular connective tissues of pig skin after irradiation. *Radiotherapy and Oncology*. 1988; 11:73–82. [PubMed: 3344355]
15. Wilson JM, Sanzari JK, Diffenderfer ES, Yee SS, et al. Acute biological effects of simulating the whole-body radiation dose distribution from a solar particle event using a porcine model. *Radiat Res*. 2011; 176:649–59. [PubMed: 21859326]
16. Zacharias T, Dorr W, Enghardt W, Haberer T, et al. Acute response of pig skin to irradiation with 12C-ions or 200 kV X-rays. *Acta Oncol*. 1997; 36:637–42. [PubMed: 9408156]
17. Ahmed EA, Agay D, Schrock G, Drouet M, et al. Persistent DNA damage after high dose in vivo gamma exposure of minipig skin. *PLoS One*. 2012; 7:e39521. [PubMed: 22761813]
18. Cengel KA, Diffenderfer ES, Avery S, Kennedy AR, et al. Using electron beam radiation to simulate the dose distribution for whole body solar particle event proton exposure. *Radiat Environ Biophys*. 2010; 49:715–21. [PubMed: 20725839]
19. Lindwall G, Hsieh EA, Misell LM, Chai CM, et al. Heavy water labeling of keratin as a non-invasive biomarker of skin turnover in vivo in rodents and humans. *J Invest Dermatol*. 2006; 126:841–8. [PubMed: 16470175]
20. Hopewell JW, Nyman J, Turesson I. Time factor for acute tissue reactions following fractionated irradiation: a balance between repopulation and enhanced radiosensitivity. *Int J Radiat Biol*. 2003; 79:513–24. [PubMed: 14530160]
21. Sanzari JK, Wan XS, Wroe AJ, Rightnar S, et al. Acute hematological effects of solar particle event proton radiation in the porcine model. *Radiat Res*. 2013; 180:7–16. [PubMed: 23672458]
22. Diffenderfer ES, Dolney D, Schaettler M, Sanzari JK, et al. Monte Carlo modeling in CT-based geometries: dosimetry for biological modeling experiments with particle beam radiation. *J Radiat Res*. 2014; 55:364–72. [PubMed: 24309720]
23. Miot HA, Brianezi G, Tamega AD, Miot LDB. Techniques of digital image analysis for histological quantification of melanin. *Anais Brasileiros De Dermatologia*. 2012; 87:608–611. [PubMed: 22892776]
24. Billings PC, Sanzari JK, Kennedy AR, Cengel KA, et al. Comparative analysis of colorimetric staining in skin using open-source software. *Exp Dermatol*. 2015; 24:157–9. [PubMed: 25393687]
25. Suzukawa AA, Vieira A, Winnischofer SM, Scalfio AC, et al. Novel properties of melanins include promotion of DNA strand breaks, impairment of repair, and reduced ability to damage DNA after quenching of singlet oxygen. *Free Radic Biol Med*. 2012; 52:1945–53. [PubMed: 22401857]

26. Kadekaro AL, Wakamatsu K, Ito S, Abdel-Malek ZA. Cutaneous photoprotection and melanoma susceptibility: reaching beyond melanin content to the frontiers of DNA repair. *Front Biosci.* 2006; 11:2157–73. [PubMed: 16720302]
27. Yamaguchi Y, Hearing VJ. Physiological factors that regulate skin pigmentation. *Biofactors.* 2009; 35:193–9. [PubMed: 19449448]
28. Hussein MR. Ultraviolet radiation and skin cancer: molecular mechanisms. *J Cutan Pathol.* 2005; 32:191–205. [PubMed: 15701081]
29. Tomita Y, Maeda K, Tagami H. Melanocyte-stimulating properties of arachidonic acid metabolites: possible role in postinflammatory pigmentation. *Pigment Cell Res.* 1992; 5:357–61. [PubMed: 1292020]
30. Tomita Y, Maeda K, Tagami H. Mechanisms for hyperpigmentation in postinflammatory pigmentation, urticaria pigmentosa and sunburn. *Dermatologica.* 1989; 179(Suppl 1):49–53. [PubMed: 2550287]
31. Rubin, EaR; H, M. *The Essentials of Rubin's Pathology.* Lippincott Williams & Wilkins; 2013.
32. Zhou Y, Ni H, Balint K, Sanzari JK, et al. Ionizing radiation selectively reduces skin regulatory T cells and alters immune function. *PLoS One.* 2014; 9:e100800. [PubMed: 24959865]

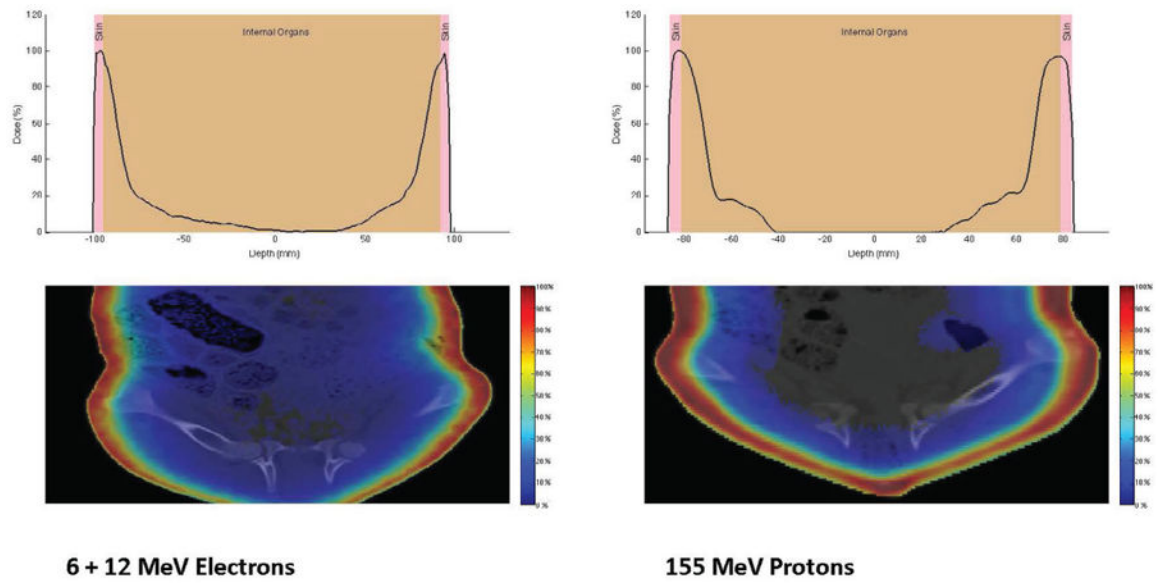


Figure 1. Dose profile of eSPE and pSPE Radiation

Top: Dose profile of the top horizontal edge of the CT-dose image (bottom panel). The dose distribution in the skin is delineated by 5 mm thick bands. Bottom: Coronal slice from a CT image of a Yucatan mini pig. The image has been cropped to the animal's rump region.

Overlaid on the CT image is a dose heat map generated by Monte Carlo simulation of the radiation beam used in this work. Left: 6 + 12 MeV eSPE radiation; Right: pSPE radiation. The dose is normalized to 100% at the depth of maximum dose.

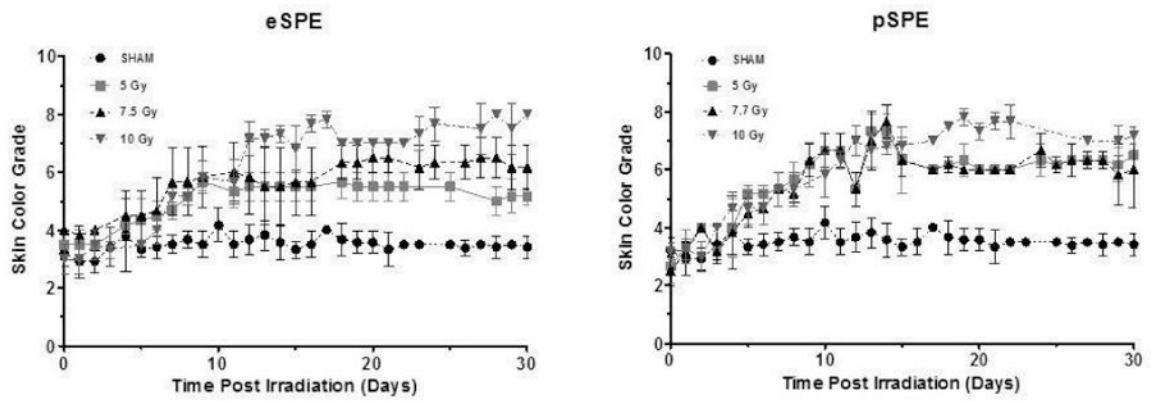


Figure 2. Radiation-Induced Hyperpigmentation

Grading of pigmentation as a function of time following radiation exposure. Animals were irradiated with eSPE or pSPE radiation and skin color was monitored using a graded scale (from 1-8) corresponding to different degrees of pigmentation. The average score was taken from 3 consistent areas on each pig per dose group ($n=3$) as shown by the mean score \pm SEM.

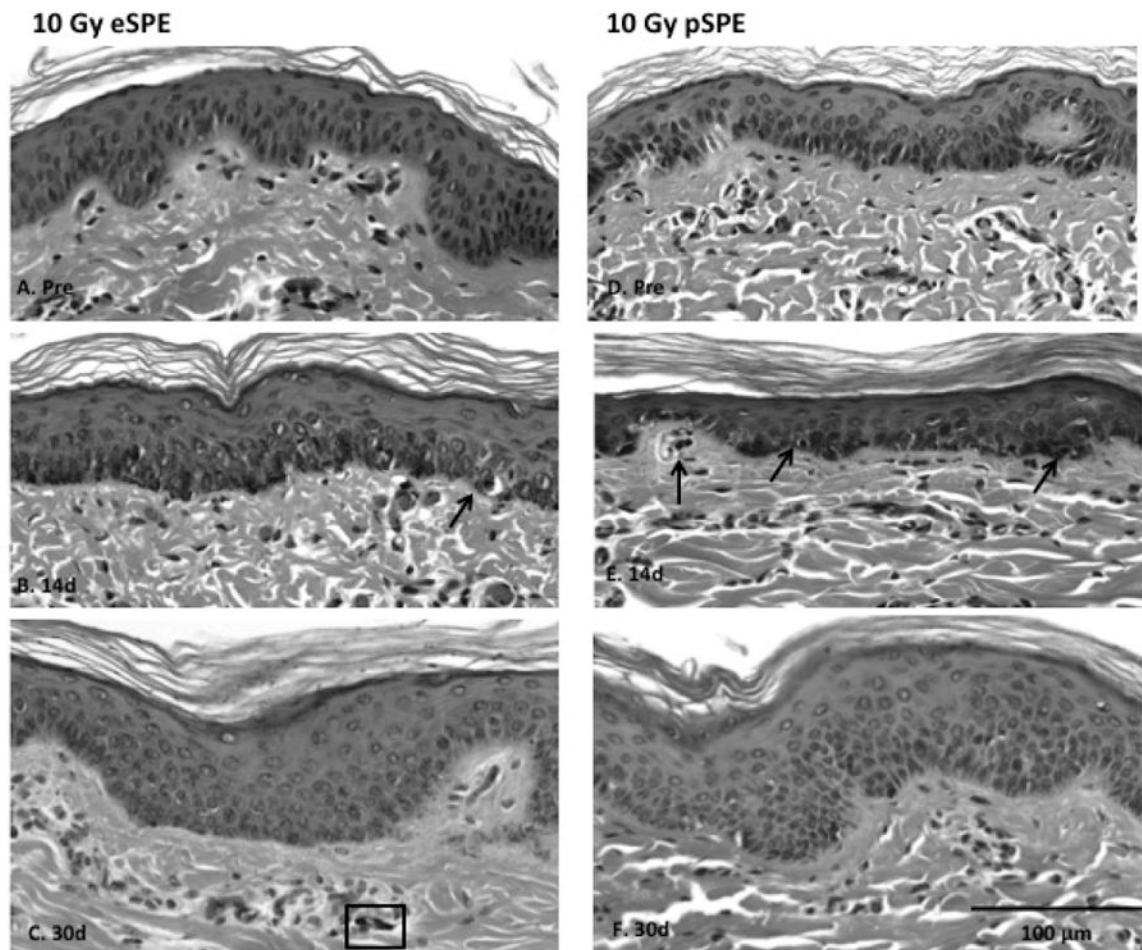


Figure 3. HE Stained Sections of Pig Skin

Skin biopsy samples were obtained pre-irradiation (Pre), 14 (14d) and 30 days (30d) following treatment with either 10 Gy eSPE (left, A-C) or 10 Gy pSPE (right, D-F). Increased deposition of melanin in the epidermis is observed following radiation exposure. To note: black arrows indicate necrotic keratinocytes; rectangular box in C. indicates a random shrunken (pyknotic) residual nuclei; white arrow in E. indicates a melanophage; solid bar, 100 μm .

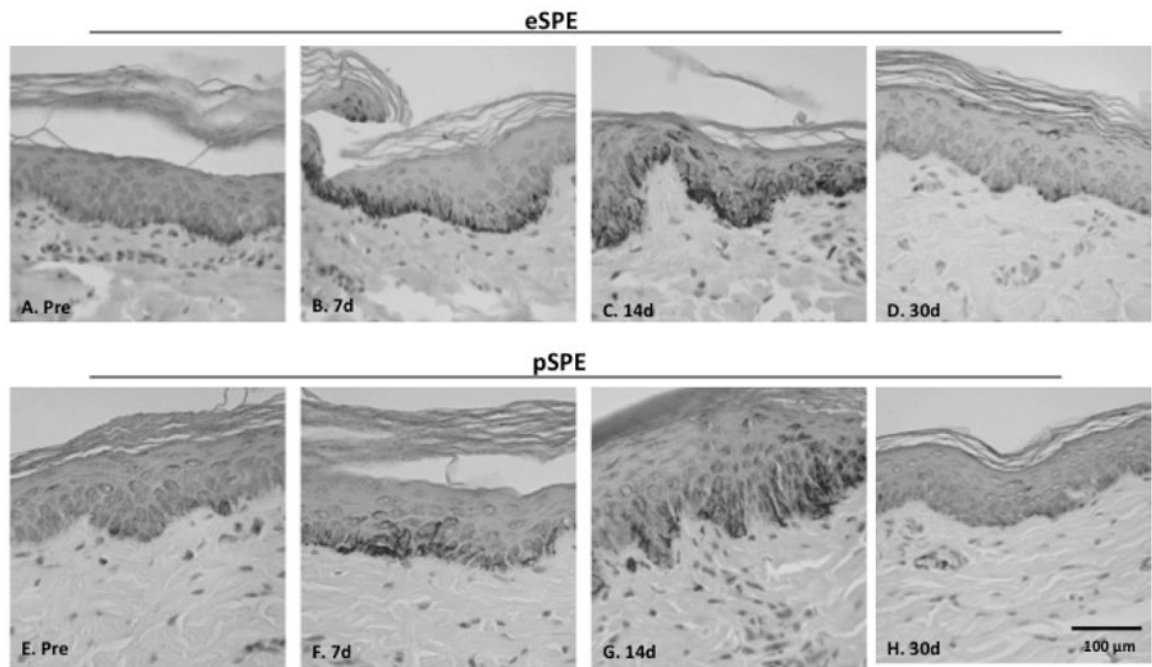


Figure 4. Fontana Masson Stained Melanin

Skin biopsy samples were obtained pre-irradiation (Pre) and at 7 (7d), 14 (14d) and 30 (30d) days post-irradiation with 10 Gy eSPE (upper) or 7.7 Gy pSPE (lower). Melanin deposition is shown with Fontana Masson staining (positive staining appears brownish-black). Increased melanin deposition is observed following radiation exposure, which is particularly prominent at 7 and 14 days post-irradiation in the basal epidermis.

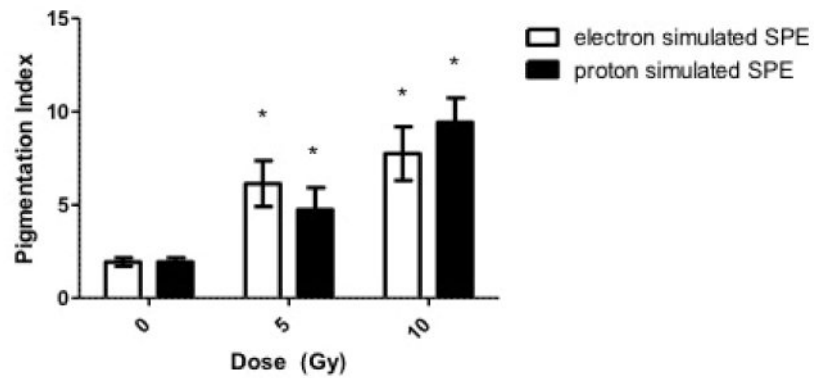


Figure 5. Melanin Quantitation

Melanin present in the epidermis was quantified in the Fontana Masson stained skin biopsy sections at the 14 day post-irradiation time point. Results are presented as Pigmentation Index, which is defined as the number of brown-black pixels present per field. Note the radiation dose-dependent increase in pigment Index. Data are presented as the mean \pm SD. The pigmentation score is increased in the irradiated biopsy samples vs. the non-irradiated biopsy samples taken prior to radiation exposure, statistical significance by the Student's t test is indicated by *, $p < 0.05$, compared to the 0 Gy (control) average.

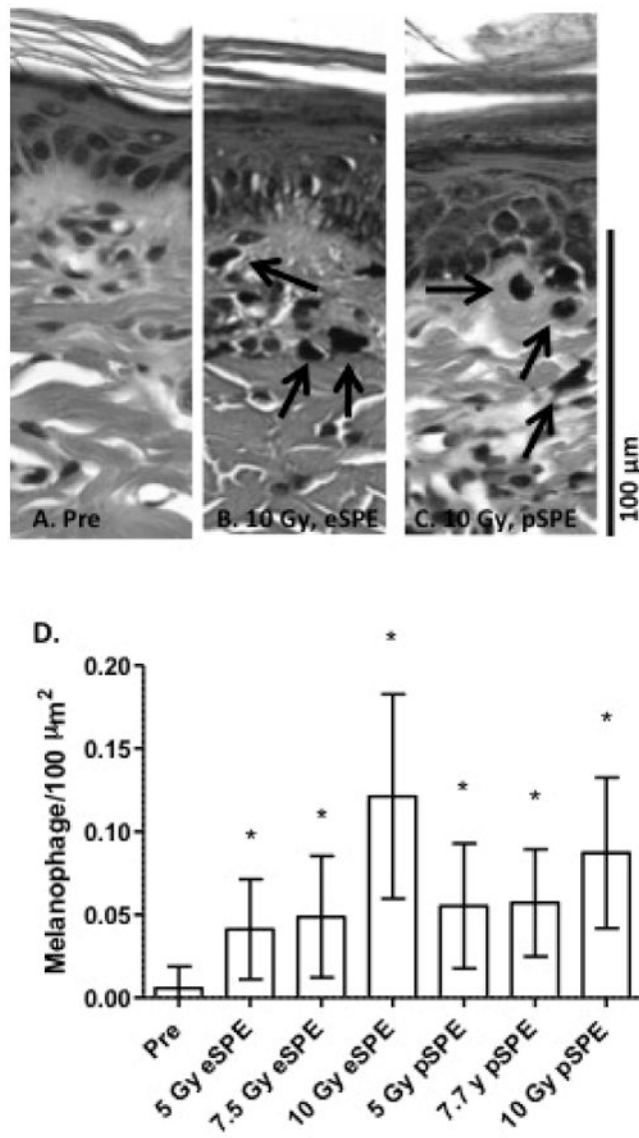


Figure 6. Presence of Melanophages

Skin samples were taken pre-irradiation (Pre, A) or at 30 days post-irradiation with either 10 Gy of eSPE (B) or 10 Gy of SPE radiation (C). Note the presence of melanophages (black arrows) in the dermis of irradiated animals. Data are presented in histogram form (D) as the number of melanophages present per unit dermal area (mean \pm SD). Statistical significance by the Student's t test is indicated by *, $p < 0.0001$.

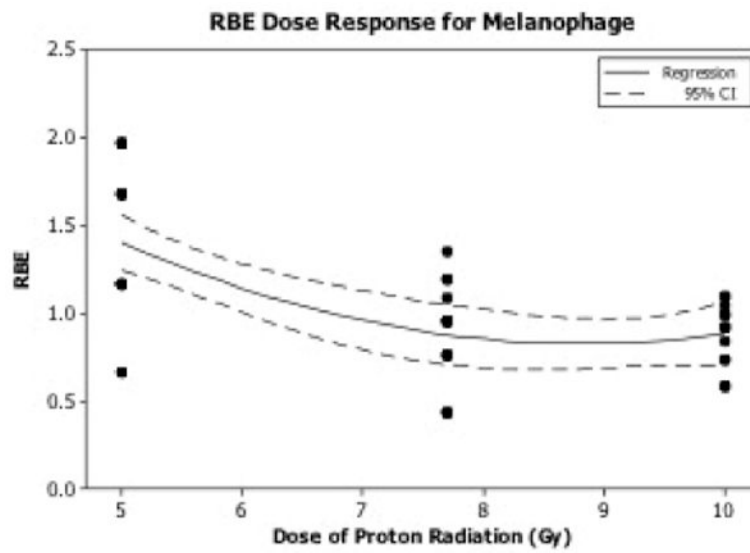


Figure 7. Relative Biological Effectiveness (RBE) of melanophage presence following irradiation
 The RBE dose response relationship for melanophage number in animals irradiated with SPE-like protons was determined. RBE values were calculated using $RBE = D_{\text{electron}} / D_{\text{proton}}$.

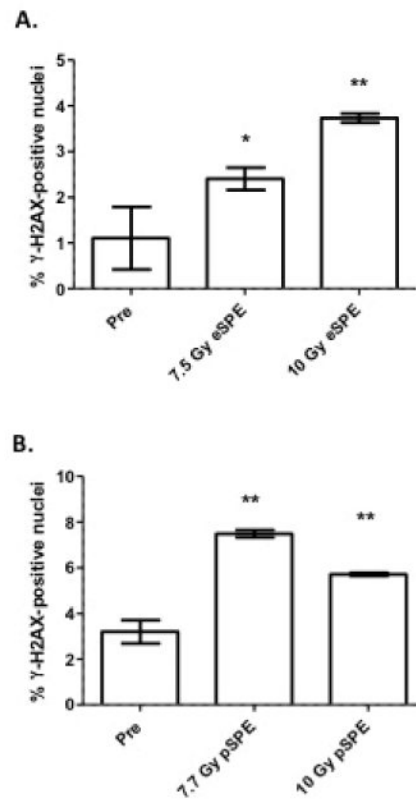


Figure 8. Radiation-induced DNA damage

The presence of γ -H2AX phosphorylation in the nuclei of skin cells was counted 7 days after either eSPE (A) or pSPE (B) exposure and compared to the average pre-irradiation (Pre) positively-stained nuclei. Data are presented as the mean \pm SD and statistical significance by the Student's t test is indicated by *, $p < 0.05$ or **, $p < 0.01$.

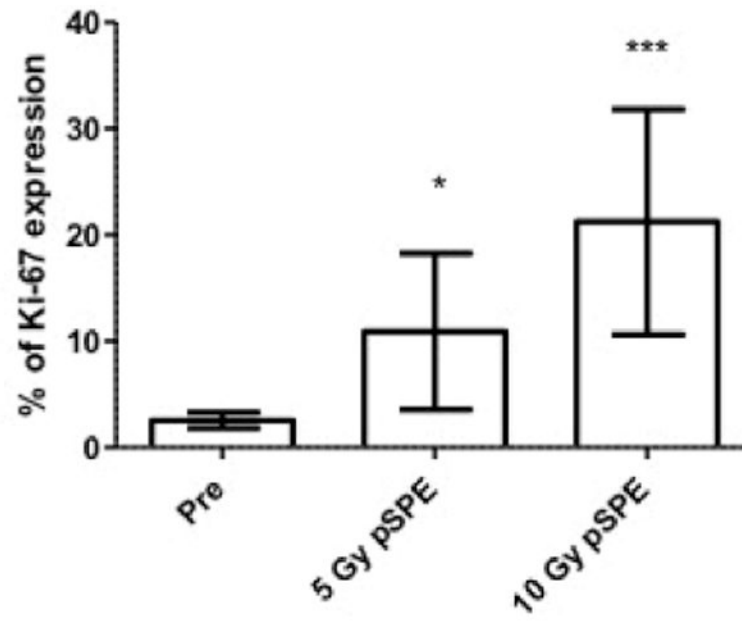


Figure 9. Assessment of epidermal proliferation

Sections from animals exposed to pSPE radiation were stained with anti-KI67, a marker of cell proliferation. Increased expression is observed 14 days after radiation exposure, compared to the average pre-irradiation samples (Pre). Statistical significance by the Student's t test is indicated by *, $p < 0.05$ or ***, $p < 0.001$.

Table 1
Animal Irradiation Conditions¹

Total Dose	Radiation¹	Dose Rate (Gy/hr)
Sham	None	0
5 Gy	eSPE	1.7
7.5 Gy	eSPE	2.5
10 Gy	eSPE	3.3
5 Gy	pSPE	5
7.7 Gy	pSPE	5
10 Gy	pSPE	5

¹Animals received total body irradiation (TBI) and were irradiated with electron (e) or proton (p) simulated SPE radiation.

Author Manuscript

Author Manuscript

Author Manuscript

Author Manuscript

Table 2

RBE for pSPE using the melanophage number as the biological endpoint.

Dose of pSPE (Gy)	RBE		
	Fitted value	95% confidence interval	
		Lower limit	Upper limit
5	1.4	1.2	1.6
7.7	0.9	0.7	1.0
10	0.9	0.7	1.1

Author Manuscript

Author Manuscript

Author Manuscript

Author Manuscript